3D Curved Slice Imaging

Hans Weber[1], Sebastian Littin[1], Gigi Galiana[2], Feng Jia[1], Anna Masako Welz[1], Robert Todd Constable[2,3], Jürgen Hennig[1], and Maxim Zaitsev[1]

[1]*Department of Radiology, Medical Physics, University Medical Center Freiburg, Freiburg, Germany,* [2]*Diagnostic Radiology, Yale University, New Haven, CT, United States,* [3]*Biomedical Engineering, Yale University, New Haven, CT, United States*

Introduction Nonlinear spatial encoding magnetic fields enable the excitation of curved slices with a conventional 1D RF-pulse. The ExLoc concept [1] describes not only the slice selection field, but also the in-plane encoding fields, which are adjusted to the object under investigation by adequate superposition of field components. The aim is a locally orthogonal orientation of the encoding fields (both for slice selection an in-plane) in order to maintain a local rectangular voxel shape. The shape of the available field components defines the range of possible slice shapes. Previous work using a PatLoc gradient insert [2], generating two second order fields (2xy, x^2-y^2), demonstrated the ExLoc concept for slices exhibiting one curved slice dimension with the latter being orientated in the xy-plane (ExLoc2D). In this study, we apply the ExLoc concept to a recently presented planar gradient system (FlatLoc [3]), generating three approximately locally orthogonal field components with nonlinear variation along all three dimensions. For the first time, this allows us to explore the excitation and geometrically matched local encoding of slices with two curved slice dimensions oriented along all three dimensions in space (ExLoc3D).

Methods All imaging experiments were performed on a 3T MAGNETOM Trio TIM system (Siemens, Erlangen, Germany) with the FlatLoc gradient system positioned on the patient table. In a first step, each field component was mapped within a half cylindrical, homogeneous phantom (radius: 220 mm, length: 530 mm) with an isotropic resolution of 3.9 mm using the linear system. Prior to conversion to field strength per unit current, the phase maps were unwrapped, filtered for noise and masked to the phantom shape.

For directed adaptation of the ExLoc3D slice shape to an arrangement of structured phantoms, slice cross-sections were simulated on basis of the field map data and overlaid on a localizer image. The final slice selection field was composed of two of three FlatLoc field components. Whereas for globally orthogonal field components (such as three conventional, linear fields, or the two PatLoc system fields) the corresponding in-plane encoding fields for a given slice selection field can be easily determined by applying rotations, this is no longer possible for field components exhibiting only local orthogonality. Therefore, the composition of both the read and phase encoding fields were determined by optimizing the fields' orientation to each other and to the slice selection field. As an optimization criterion (OC), the "cross dot product" of the normalized local gradient vectors of all three encoding fields $\mathrm{OC}(\mathbf{x}) = \left\{ \left(\mathbf{G}_R(\mathbf{x}) \times \mathbf{G}_P(\mathbf{x}) \right) \cdot \mathbf{G}_S(\mathbf{x}) \right\}$ was chosen. A maximum possible OC value of one corresponds to an orthogonal orientation. The dot product decreases as gradient orientations move further away from the orthogonal orientation. Within the optimization process, the local OC value for each point within the slice volume was evaluated and its average value maximized by varying the fields' composition using a direct search method in Matlab (The MathWorks, Natick, USA).

The optimized field compositions were used in a spin-echo sequence for acquisition of the ExLoc3D image (Matrix: 256 x 256; TR/TE: 1000/100 ms). Fourier transform of the acquired data yielded the image in distorted encoding space coordinates. Transformation into the undistorted object space was performed as described in [1] by iteratively solving the equation that describes the relation between encoding and object space coordinates. Basically, the field mapping data provide this relation between both spaces.

Results and Discussion Figure 1 shows the cross-section of the acquired 3D field maps for each component of the FlatLoc system. As expected, the field strength increases near the coil windings. Component 1 exhibits a dome like shape, whereas the other two components generate their strongest variation along the x and z dimensions, respectively. The simulated cross-section of the slice after adaptation to the phantom is presented in Fig. 2 and shows the curvature of the slice along both slice dimensions. The acquired ExLoc3D image in distorted encoding space coordinates is displayed in Fig. 3. The very low intensity variations are consistent with the almost constant slice thickness already observed in the simulations (Fig. 2). The final ExLoc3D image in object space coordinates is shown in Fig. 4. The varying shape of the tubes' cross-sections (most prominent in the front center part) is in accordance with the determined slice orientation. Within a stripe located at the x center with orientation along the z dimension, the structures appear sharper.

Transformation from encoding to object space took on average approximately 2.4 sec per voxel on a standard desktop PC, resulting in total reconstruction time of about 160 min. This duration results from the fact that the high-resolution 3D field maps have to be interpolated for each iteration. An analytical description of the FlatLoc fields could avoid the interpolation process but due to coil imperfection this would have insufficient accuracy. This is especially true for voxels located close to the border of the field map volume, where interpolation fails and this dramatically increases the reconstruction time. However, due to the fields' smoothness, it appeared to be sufficient to transform only every fourth voxel and to determine the remaining object space positions by interpolation. Figure 5 depicts the resulting local OC values within the slice volume for the optimized encoding field combination. Within the center, there is a large area with values greater than 0.8. This corresponds to an average deviation of each gradient of 15° or less from an orthogonal orientation. The average OC value over the total slice volume of 0.6 corresponds to 25°, respectively. The lack of global orthogonality of the FlatLoc fields eliminates the possibility of achieving an orthogonal encoding field orientation across the whole slice volume. However, by reducing the optimization volume to an ROI, the local best encoding can be determined.

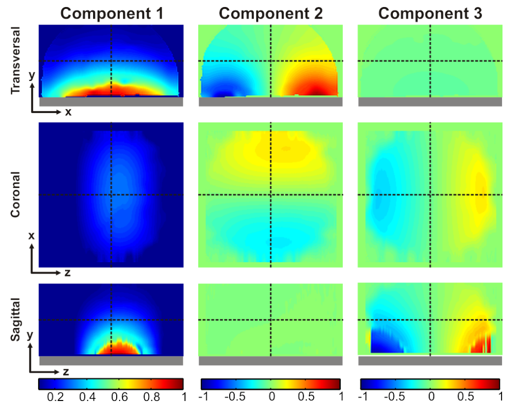

Fig. 1: Selected cross-sections of the (normalized) FlatLoc field maps. The dotted lines describe the intersections of the cross-sections.

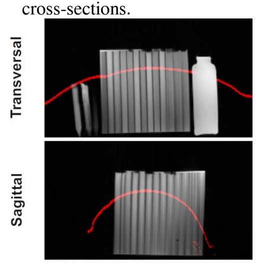

Fig. 2: Localizer images with simulated cross-sections of the slice.

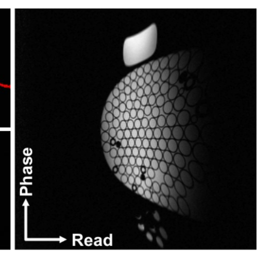

Fig. 3: ExLoc3D image in distorted encoding space co-ordinates after Fourier trans-formation of the raw data.

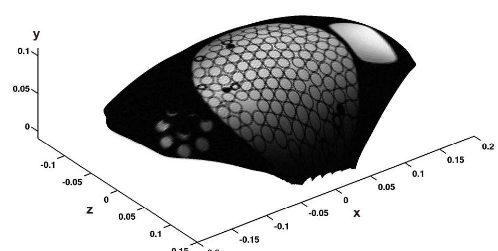

Fig. 4: Final ExLoc3D image after transformation into undistorted object space coordinates. The shape of the tubes' cross-sections matches with the orientation of the slice.

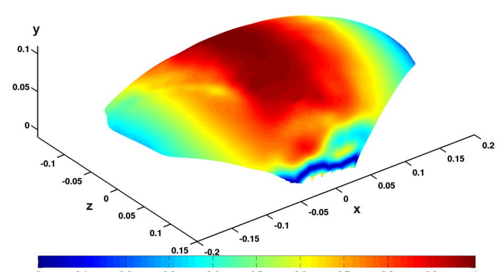

Fig. 5: Map of the local OC values within the slice volume. Decreasing OC values towards the periphery correspond to a deviation of the local encoding field gradients from orthogonality.

Conclusion This study demonstrates that, with adequate field component selection, excitation and geometrically matched local encoding of slices with two curved slice dimensions, (ExLoc3D) is feasible. As such fields typically do not exhibit global orthogonality, optimization of the in-plane encoding field composition is required. The usage of additional linear field components may increase the area of orthogonal field orientation.

Acknowledgement This work was supported by the European Research Council Starting Grant 'RANGEMRI' grant agreement 282345 and by a fellowship of the German Academic Exchange Service.

References [1] H. Weber et al., MRM 2012, doi: 10.1002/mrm.24364; [2] A. Welz et al., Proc. ESMRMB 2009, #316; [3] S. Littin et al., Proc. ISMRM 2012, #698;